

A Variable Degree-of-Freedom and Self-sensing Soft Bending Actuator Based on Conductive Liquid Metal and Thermoplastic Polymer Composites

Yufei Hao¹, Zemin Liu¹, Zhixin Xie¹, Xi Fang¹, Tianmiao Wang^{1,2}, Li Wen^{1,2*}

Abstract— This paper presents a soft actuator embedded with conductive liquid metal and shape memory epoxy (SME) which function together to enable self-sensing, tunable mechanical degrees of freedom (DoF), and variable stiffness. We embedded thermoplastic shape memory epoxy in the bottom portion of the actuator. Different sections of the SME could be selectively softened by an implanted conductive silver yarn located at different positions. When an electric current passes through the conductive silver yarn, it induces a phase transition that changes the epoxy from stiff state to compliant state. Each section of SME could be softened within 5 s by applying a current of 200 mA to the silver yarn. To acquire the strain curvature, eGaIn was infused into a microchannel surrounding the chambers of the soft actuator. A spiral-shaped eGaIn sensor was also attached to the tip of the actuator to perceive the contact with reliable dynamic force response. Systematic experiments were performed to characterize the stiffness, tunable DoF, and sensing property. We show the ability of the soft composite actuator to support a weight of 200g at the tip (as a cantilever) while maintaining the shape and the ability to recover its original shape after large bending deformation. In particular, seven different motion patterns could be achieved under the same pneumatic pressure of the actuator due to selectively heating the SME sections. A gripper which was fabricated by assembling two actuators to a base was able to grasp the weight up to 56 times of a single actuator through an appropriate motion pattern. For demonstration purposes, the gripper was used to grasp various objects by adjusting the DoF and stiffness with real-time feedback of the bending strain and the contact force.

I. INTRODUCTION

Compared to rigid robots, soft robots demonstrate several overwhelming advantages such as deforming in confined space [1], absorbing energy in collisions [2] and interacting safely with the surroundings [3] due to the intrinsically soft and adaptable properties. Soft robots can be actuated by various approaches: compressed fluids [4], chemical reaction [5] and smart materials such as SMA [6]. Among these actuators, pneumatic/fluidic elastomeric actuators showed remarkable flexibility and dexterity for gripping application even under very simple control [7]. However, the low stiffness of the elastomer impedes further load applications of the soft actuators. The monotonous motion configuration under pneumatic/hydraulic actuation also limits the capacity of executing effective and complex works by soft robots. To solve these issues, the research on the variable degrees of

freedom (DoF), stiffness tuning and soft deformable sensors is imperative.

To achieve multiple degrees of freedom, some researchers mechanically increased the serial or parallel pneumatic/fluidic channels that can be separately pressurized [8]. Although some works integrate the elastomeric actuator with functional materials, such as fibers [9], paper [10], and fabric patches [11] to alter the monotonous motion pattern, these types of actuators were still limited to one motion configuration, i.e., the DoF remain unchanged. To alter or enrich the DoF of the actuator during operation, researchers incorporate the stiffness-tuning materials into soft actuators, which can alter their stiffness under the external stimulus. For example, by softening the shape memory polymers [12], low melting point alloys [13] or conductive elastomers [14] which are located in preset locations of the soft robots.

Until now, several types of soft sensors have been developed that can be integrated into soft robots. For example, the tiny magnet was embedded in the body of soft actuators to acquire the curvature information [15]. The stretchable optical waveguides sensor was used for strain sensing of the prosthetic hand [16]. Some researchers also attempted to make soft sensors using flexible conductive materials such as the capacitive strain sensors made of the conductive fabric [17] and PDMS with carbon [18], etc. Besides, eGaIn, which is metal but in the liquid state under room temperature, can be easily injected into the body of soft robots and have infinite ductility as long as the body of soft robots is functional. Therefore researchers fabricated eGaIn based soft sensors to sense the strain [19], normal pressure [20], tactile [21] or multi-axis force [22]. Moreover, eGaIn sensors have been investigated extensively in soft robots [23]-[25]. Therefore, it would be promising to integrate the eGaIn sensor into a soft actuator that has multiple DoF and variable mechanical stiffness.

In this paper, we present a soft actuator embedded with conductive liquid metal and shape memory epoxy (SME) which function together to enable self-sensing, tunable mechanical degrees of freedom (DoF), and variable stiffness. The shape memory epoxy was used to fabricate the DoF change layer at the bottom of the soft actuator. We can soften different sections of the SME by adding electric currents through the conductive silver yarn fabric. Upon heating, the stiffness of the sections was also changed, and the corresponding sections of the actuator can bend upon inflation (cannot bend while unheated). Furthermore, eGaIn sensors were embedded in the actuator to sense the position and force information. Systematic experiments were performed to characterize the stiffness,

This work was supported by the National Science Foundation projects, China under contract number 61333016 and 61633004. Authors are with the School of Mechanical Engineering and Automation¹, and Beijing Advanced Innovation Center for Biomedical Engineering², Beihang University, Beijing, 100191, People's Republic of China; please e-mail Prof. Li Wen for contact: liwen@buaa.edu.cn).

tunable DoF, and sensing property. Finally, a two-fingered gripper was fabricated to demonstrate the variable DoFs and sensing ability of the actuator while grasping objects.

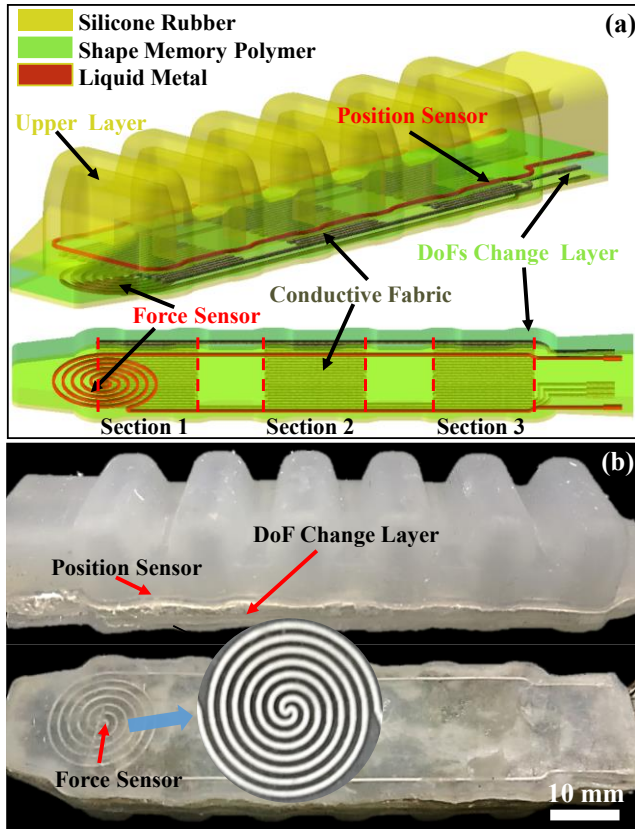


Fig. 1. The design of the multi-functional soft actuator prototype. (a) The three-dimensional model shows that the actuator is composed of two functional layers: The upper layer for pneumatic actuation and the bottom layer for tuning the degree-of-freedom. To acquire the curvature information of the actuator during bending, the eGaIn channel is embedded into the upper layer. The bottom layer was fabricated with shape memory epoxy, with conductive silver yarn implanted into the different sections of the layer. A spiral-shaped eGaIn force sensor was attached to the tip of the actuator to perceive force when contacting with objects. Note that different colors represent different materials. (b) The snapshots of the actuator prototype. Scale bar is 10 mm.

II. MATERIALS AND METHODS

A. Design and Fabrication of the Soft Actuator

The detailed structure of the soft actuator is illustrated in Fig. 1. As Fig. 1 shows, the soft actuator mainly contains the upper layer and the DoF change layer. The upper layer was a typical ribbed structure which is easy to fabricate. To get the position information, a microchannel with a cross-section of 0.3 mm and 0.3 mm, which was filled with eGaIn (Sigma-Aldrich Inc., USA), was designed to surround the chambers of the top layer (shown in Fig. 1(a)). After calibrating the relationship between the resistance and the curvature of the actuator under different pressures, the sensor could be used to feedback the position information. The DoF change layer was mainly made of the shape memory epoxy [26], which is a composite of EPON 828 and Jeffamine D400. Moreover, the stiffness of the composite could be changed when heated above the glass transition temperature

44°C [26]. Thus a conductive silver yarn with a diameter of 0.3 mm was embedded inside the DoF change layer to directly heating it. Furthermore, the silver yarn was embedded only in three sections of the DoF change layer. Thus the actuator will have various configurations by adding current to the different sections. Based on the combination theory, the actuator will have seven motion patterns ($c_3^1 + c_3^2 + c_3^3$) by melting the different sections, with only one air channel is provided, which was well demonstrated in Fig. 2. **To demonstrate the tunable DoFs, in supplementary video part 1 we show all the seven motion patterns the actuator achieved.** To acquire the force information, the eGaIn force sensor inspired by [20] was also put at the bottom of the DoF change layer. The dimension of the microchannel is 0.3 mm × 0.3 mm.

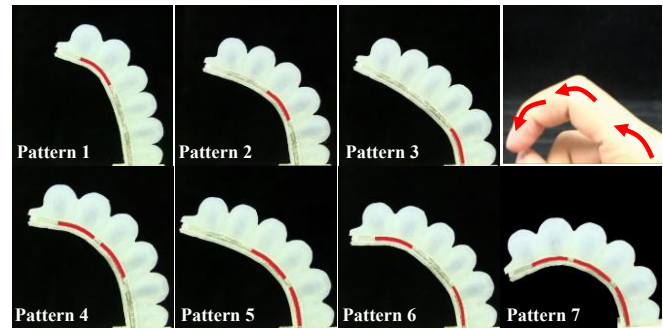


Fig. 2. The seven motion patterns of the soft composite actuator when different sections of the DoF change layer were heated by applying a current to the conductive silver yarn. All the motion patterns were achieved under the same air pressure (45 kPa). **These motions were also shown in supplementary video part 1.**

The fabrication of the actuator was a layered up method, with the individual parts fabricated first and glued together from bottom to top. The upper layer and the force sensor were fabricated using the multi-step molding process method [3], and eGaIn was injected into the microchannels via the syringe vacuum methods [20]. All the molds were 3D printed using epoxy, and the silicon rubber used was Dragon Skin 20 (Smooth-on Inc., USA). To fabricate the DoF change layer, the two composites, i.e., EPON 828 (Hexion Inc., USA) and Jeffamine D400 (Huntsman Polyurethanes Ltd, China) were first mixed at a ratio of 10:4 by weight [27], then let sit for about 24 hours to release the bobbles and increase the viscosity. After that, the mixture was poured into the silicone rubber mold and cured for about six hours at 70°C. After twining the conductive silver yarn at the three sections, the uncured composite was poured above the yarn and cured at the room temperature for about 24 hours. Thus the heater was embedded into the inner of the DoF change layer to speed up the glass transition process. It should be noted that the DoF change layer must not be heated to cure after the conductive fabric was embedded. Because the unbalanced internal stress may cause the structure to deform under heating. After all the components were fabricated, they were glued together via QIS-3009 (DongGuan JingDa Adhesive Co., Ltd, China).

B. Experiments on the Position Sensor

To evaluate the ability of the position sensor, two experiments were conducted. The first experiment was to test the performance of the sensor under different motion patterns

and air pressures. For this experiment, we first fixed the actuator to a base, then softened the corresponding sections to achieve the seven motion patterns. For each motion pattern, the actuator was inflated with increased pressures starting from 5 kPa to 40 kPa with an interval of 5 kPa to test the sensor responses. The pressure was controlled by the electric proportional valve (ITV0030, SMC, Japan). The change of the resistance of the sensor was recorded via a precision multimeter (Fluke 8845A, Fluke Inc., USA). For each pressure, three trials were conducted, and the average variation of the resistance was obtained. The second experiment was to test the dynamic response and the robustness of the position sensor. For the aim, we inflated the actuator with a trapezoidal function of pressure in different periods. The peak of the function was set to 35 kPa. During the inflation, the change of the resistance and the pressure were simultaneously recorded via the NI data acquisition board (PCI-6284, National Instruments, USA). To measure the resistance of the sensor, a constant current of 100 mA was applied to the sensor, and the relative voltage increment was obtained to calculate the resistance. To measure the simultaneous value of the pressure, a pressure sensor (ISE30A-01-C, SMC, Japan) was connected to the air flow through the one-touch fitting (KQ2LU04-00A, SMC, Japan).

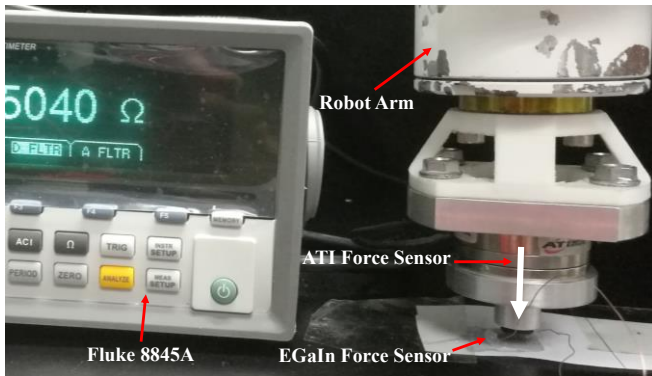


Fig. 3. The experimental setup for the EGaIn force sensor, an ATI force transducer was mounted on the robotic arm. The resistance of the eGaIn is acquired by Fluke 8845A.

C. Experiments on the Force Sensor

A setup was established to evaluate the ability of the force sensor. As Fig. 3 shows, the force sensor was fixed to the desk by the adhesive tape to avoid slippage during the experiment. The sensor was wired to Fluke 8845A. A rigid round stamp with a diameter of 9 mm was used to press and exert a force on the sensor. The base of the stamp was fixed to the six-axis force transducer (Mini 40 F/T sensor, ATI, USA) which was fastened to a robot arm (MOTOMAN MH3F, YASKAWA Inc., Japan) moving vertically. On this setup, three experiments were conducted to test the performance of the force sensor. The first experiment was to calibrate the force and the electrical resistance. During the process, the robot arm was programmed to move downward in 0.03 mm step from 0 to 0.3 mm (the height of the chamber) at a speed of 0.3 mm/s. Between two adjacent steps, there was a four seconds pause. The resistance's change was recorded via Fluke 8845A, and the Ni board recorded the force data simultaneously. Because the force and the resistance were obtained under the same displacement, we finally obtained the relationship between the

force and resistance. Three trials were conducted to get the average trend. The second experiment was to characterize the dynamic response of the sensor under different press speeds. The robot arm was programmed to indent the sensor from 0 to 0.3 mm at the speeds of 0.5mm/s, 1 mm/s and 2 mm/s respectively. To get the instantaneous change of the resistance, the sensor was energized with a current of 100 mA and the voltage of the sensor was recorded via the NI board. The last experiment was to test the repeatability of the sensor. The robot arm was programmed to exert two square waves with amplitudes of 0.03 mm and 0.3 mm. The speed of the robot arm was 5 mm/s while the suspension of each movement was 4 seconds.

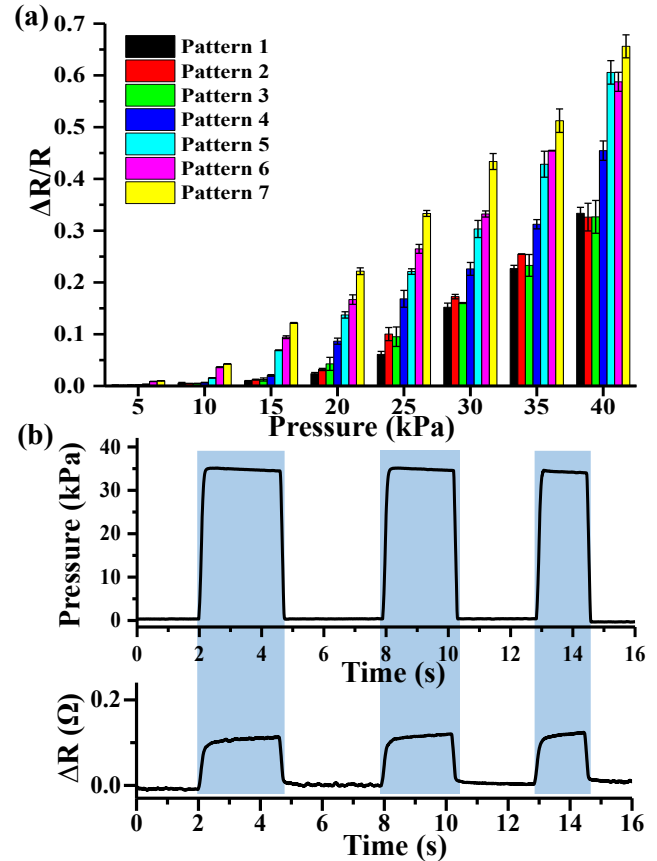


Fig. 4. The experiment resistance of the bending sensor under different motion patterns. (a) The resistance variation of the sensor under different pressures (0-40kPa) and the seven motion patterns of the soft actuator (see Fig. 2 for notation). (b) The response of the sensor when the actuator (at the motion pattern 2) was inflated under different pneumatic actuation cycles. The pneumatic pressure was 35 kPa.

D. Application Evaluation

For application demonstration, we fabricated a two-fingered gripper by assembling two soft actuators to a base and evaluate the grasping performance of the gripper by grasping objects with different sizes and shapes. Furthermore, we also test the sensor response of the gripper while grasping objects. For the sensor feedback test, the gripper was fixed to a base with the fingers pointing up. An octagonal prism was fixed to the robot arm, collinear with the gripper in the perpendicular direction. During the grasping, the gripper was first heated to soften the DoF change layer and inflated to

enclose the object; then the robot arm moved upwards at a speed of 2 mm/s until the object was detached from the gripper. The outputs of the position sensor and the force sensor were recorded via the NI board during the overall process for further analysis.

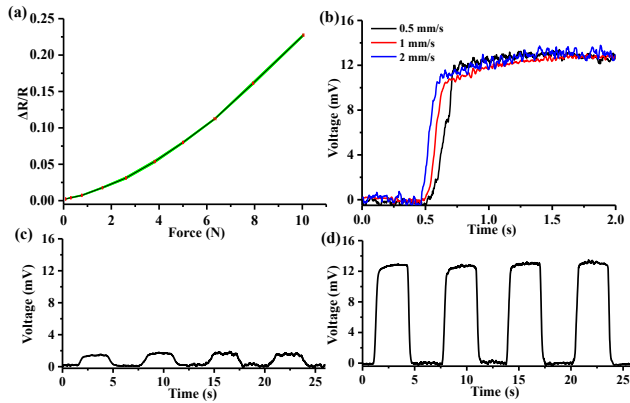


Fig.5. The experiment results of the force sensor. (a) the resistance variation as a function of the force which measured by ATI force transducer. (b) The dynamic response of the force sensor under different speeds, with the same amplitude of 0.3 mm. (c) The periodic response of the sensor under the amplitude of 0.03 mm. (d) The periodic response of the sensor under the amplitude of 0.3 mm.

III. RESULTS

A. Results of the Position Sensor

The results of the position sensor are shown in Fig.4. As Fig.4 (a) shows, for each motion patterns, the resistance of the sensor increased with the air pressure. Because the actuator bent more under bigger pressures, causing the cross-section area of the microchannel of the sensor to decrease and the length to increase. Under the same pressure, it can be seen that the change of resistance can be divided into three groups based on the heated sections of the actuator. Pattern 1, 2 and 3 were in the smallest group because only one section was heated. So the resistances of these patterns were similar. Pattern 4,5 and 6 were in the middle group. The resistances were much bigger than the previous group because two sections were heated. The resistance of pattern 7 was the biggest because all the sections were heated. In the middle group, it is obvious that the resistance of pattern 4 is smaller than the others. We hypothesize that the sensor in section 3 is sensitive than other sections, but more data should need to explain it. From Fig.4 (b), it can be seen that the resistance of the sensor kept pace with the change of the pressure for all the periods, which demonstrated that the sensor has good dynamic response and repeatability. Focusing on the step signal, we can see that there is a tiny increase in the resistance while the pressure was stable, which may be due to the hysteresis of the air during inflating.

B. Results of the Force Sensor

The dynamic stability and repeatability of the force sensor were presented in Fig.5. Fig.5 (a) shows the change of resistance as a function of force. It is obvious that the resistance presented an upward trend when the force increased. Besides, a minimum force of 0.089 N was detected

when the resistance increased 1.37 m Ω (the robot arm moved 0.03mm under this circumstance). We defined this value as the resolution of the sensor because the response of the sensor was chaotic if the robot arm moved in a smaller step. The stability of the sensor under this minimum value can be verified in Fig.5(c), which demonstrated that the sensor kept the same amplification under all the cycles. Fig.5(b) shows the response of the sensor under different press speeds. It can be seen that the resistance of the sensor increased faster when the robot arm moved faster. Furthermore, there is no big difference between the voltage changes of the sensor at all the speeds, which can demonstrate the stability of the sensor. From Fig.5(c) and (d), we can see that the voltage repeated the same trend for both the amplitudes (0.03mm and 0.3 mm), which can verify the repeatability and robustness of the sensor.

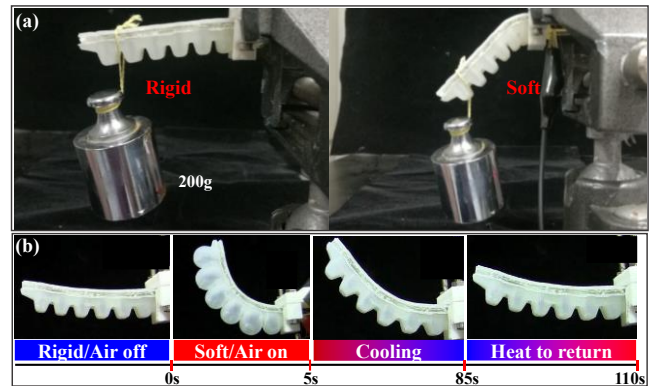


Fig.6. The demonstration of the shape-maintaining and shape-recovering properties of the soft actuator. (a) The stiffness comparison when the DoF change layer was in the rigid state and soft state when a load (200 g) is applied to the tip of the actuator. (b) The thermal response and shape memory property of the actuator. The SME could be softened in only 5 seconds with a small current of 200mA and cooling down in 80 seconds. With the shape memory property, the actuator can be heater to return to the initial state. **The whole heating and cooling process were demonstrated in supplementary video part 2.**

C. Results of the Application Evaluation

Fig.6 demonstrated the mechanical and thermal property of the actuator. As Fig.6(a) shows, when the shape memory epoxy was in the rigid state, the actuator could support a weight of 200g at the tip while maintaining the shape. Furthermore, if the material was in a soft state, it will not affect the flexibility of the actuator. It can be seen from Fig.6(b) that the actuator can be inflated to bend within 5 seconds by heating the DoF change layer with 200 mA current. When the layer was cooled down, which took about 85 seconds under the natural condition, the actuator can keep the inflated shape even when the pressure was released. Besides, by heating the layer, the actuator can return to the initial state under zero external force, which shows that the actuator also has the shape memory property. **In supplementary video part 2, we demonstrated the thermal property and shape memory property of the actuator.**

Fig.7 (a) presents the grasping ability of the gripper. By changing the motion patterns of the gripper, it can fully conform the objects, thus increasing the grasping stability. As the figure shows, the gripper can grasp objects with different

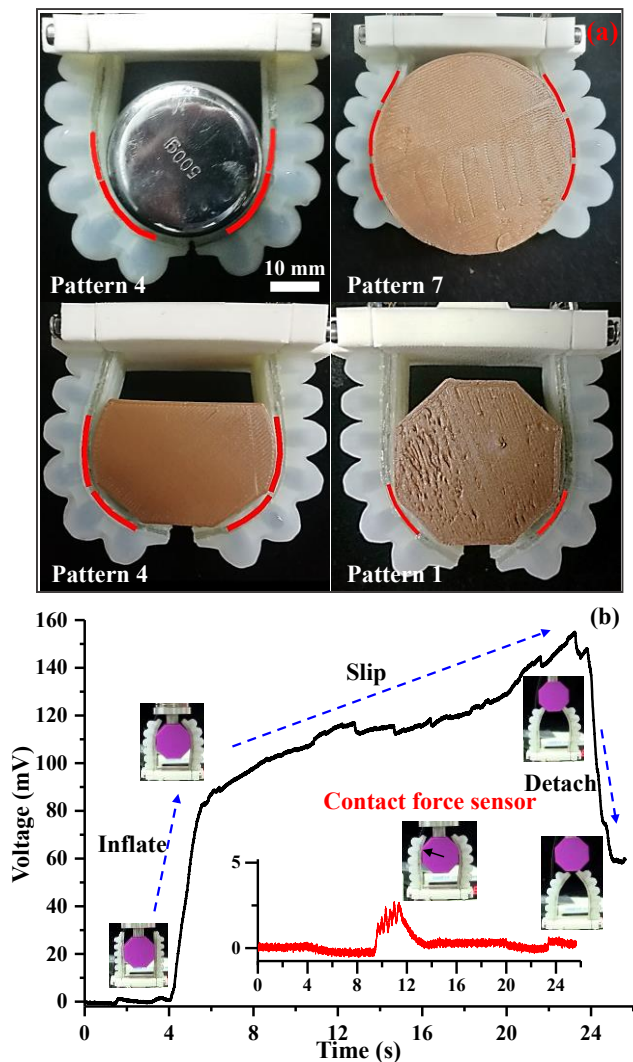


Fig. 7. The grasping demonstration of the soft gripper and the feedback of the bending sensor and force sensor. (a) The gripper can fully enclose the objects with various sizes and shapes by using different motion patterns. (b) The feedback of the position sensor and force sensor when an object is pull-off from a two-fingered gripper, the bending sensor feedback was recorded throughout the whole process (grasp->slip->detach). While the inset panel shows the results of the force sensor during this process. **The grasping process was also shown in the supplementary video part 3.**

shapes by selecting the motion patterns based on the contours of the objects (upper panels of Fig. 7 (a)). It can also fully enclose objects with different sizes by selecting the grasping actuator lengths (lower panels of Fig. 7 (a)). Furthermore, by increasing the stiffness of the actuator, the gripper could easily grasp an object of 500g (The first panel in Fig. 7(a)), which is about 56 times of the weight of an actuator (9g). This load capacity is impossible for a pure elastomer actuator. Fig. 7(b) shows the real-time feedback of the position sensor and force sensor during the grasping process. It could be seen that the position sensor responded synchronously during the whole grasping procedure. When inflating the actuator to grasp the object, the voltage of the position sensor increased sharply, which could be used to feedback the position of the gripper. During the slip stage, the voltage also increased gradually, which may be because the curvature of the actuator varied as the gripper contacted different areas of the object. When the

object was detached from the gripper, the voltage decreased. This process demonstrated that the position sensor could reflect the whole grasping process and the curvature was different when the gripper was in no-load and load conditions (under the same pressure). Besides, the force sensor also increased when the sensor contacted the object, which could be verified by the subpanel. **In supplementary video part 3, we recorded the response of the sensors during the whole grasping process.**

IV. CONCLUSION AND DISCUSSION

In summary, we have demonstrated a multi-functional soft actuator embedded with conductive liquid metal and shape memory epoxy (SME) which function together to enable self-sensing, tunable mechanical degrees of freedom (DoF), and variable stiffness. We show the ability of the soft actuator composite to bear a 200g weight as a cantilever while maintaining the shape, and to recover its original shape within 25 s via the shape memory effect. In particular, seven different motion patterns could be achieved under the same pneumatic pressure of the actuator due to selectively heating the SME sections. By using this technique, we also show that a two-fingered soft gripper can grasp various objects by adjusting the DoF and stiffness with real-time feedback of the bending strain and the contact force. Besides, by increasing the stiffness of the actuator, the gripper could grasp an object which has a weight about 56 times of a single actuator.

To achieve multiple degrees of freedom of the soft actuator through the conventional approach, separated chambers with individual pressure values are required for each DoF [7]. Reducing the size of the actuator to small-scale (while maintaining multiple DoFs) with multiple chambers is very challenging. Meanwhile, the additional pressure regulators and pneumatic air pumps can be bulky in scenarios that the overall size and weight of the soft robotic system are confined. Selectively heating the shape memory epoxy through the embedded flexible conductive fabric which induces a phase transition that changes the polymer from its rigid state to its soft state within 5 s, our soft actuator achieved seven different motion pattern under the same pneumatic pressure. Due to the low glass transition temperature of SME, the system only requires low power input for the entire system to modulate the stiffness. We also found that the cooling time of the shape memory epoxy (80 s) is significantly shorter than the low melting point alloy (300 s) [13]. To further reduce the cooling time, the hydraulic actuation method could be used because the cold water can quickly absorb more heat. Compared with the traditional multiple DoF mechanisms including rigid servo motors[28], multiple pneumatic/hydraulic sections [8], cable tendon driving[29], etc., we believe that the proposed selectively heating the shape memory epoxy (SME) approach is more compact, lightweight, cheaper and faster to fabricate.

To improve the sensory ability of the soft actuator, two eGaIn sensors (position sensor and force sensor) were embedded in the actuator. Compared with the traditional flexible sensors [30], eGaIn sensors could be casually stretched or twisted as long as the structure of the actuator is durable. Thus it is more applicable for the large deformation

soft robots. In the paper, the stability, repeatability and dynamic response of the eGaIn sensors were well demonstrated. By combining the position sensor and force sensor, the gripper can also feedback the whole grasping process of enclosing, slipping and detaching, which demonstrated the practicability of eGaIn sensors and pave the way for the automatic operation of the soft gripper with feedback control. However, a drawback exists for the position sensor because it has similar increment when the same number of sections were heated, which means that the sensor can only be used under the condition that the motion pattern is known. For the reverse application, using the sensor to estimate the motion patterns, more position sensors should be added to the actuator. Moreover, the resistance of the eGaIn sensors also increased when the heater works, but the increment was tiny (about 0.025 of the initial value at the temperature of 45 °C) and has a small influence on the precision.

For the future work, we will focus on the conductive liquid metal and shape memory epoxy (SME) integrated soft robotic gripper with visual feedback and compact control hardware that can make decisions in real-time.

ACKNOWLEDGMENT

Many thanks to Bohan Chen for the kind help in implementing the experimental apparatus.

REFERENCES

- [1] Connolly F, Polygerinos P, Walsh C J, et al. "Mechanical Programming of Soft Actuators by Varying Fiber Angle," *Soft Robotics*, vol. 2, no. 1, pp. 26-32, Mar. 2017.
- [2] Seok S, Onal C D, Cho K J, et al. "Meshworm: A Peristaltic Soft Robot With Antagonistic Nickel Titanium Coil Actuators," *IEEE/ASME Transactions on Mechatronics*, vol. 18, no. 5, pp. 1485-1497, Jul. 2013.
- [3] Hao Y, Gong Z, Xie Z, et al. "A Soft Bionic Gripper with Variable Effective Length," *Journal of Bionic Engineering*, vol. 15, no.2, pp. 220-235, 2018.
- [4] Gong Z, Xie Z, Yang X, et al. "Design, Fabrication and Kinematic Modeling of a 3D-motion Soft Robotic Arm," in *IEEE International Conference on Robotics and Biomimetics*, 2016, pp. 509-514.
- [5] Bartlett N W, Tolley M T, Overvelde J T, et al. "A 3D-printed, functionally graded soft robot powered by combustion," *Science*, vol. 349, no. 6244, pp. 161, Jul. 2015.
- [6] Lin H T, Leisk G G, Trimmer B. "GoQBot: a caterpillar-inspired soft-bodied rolling robot," *Bioinspiration & Biomimetics*, vol. 6, no. 2, pp. 026007, Apr. 2011.
- [7] Martinez R V, Branch J L, Fish C R, et al. "Robotic Tentacles with Three-Dimensional Mobility Based on Flexible Elastomers," *Advanced Materials*, vol. 25, no. 2, pp. 205-212, Sep. 2013.
- [8] Drotman D, Jadhav S, Karimi M, et al. "3D printed soft actuators for a legged robot capable of navigating unstructured terrain," in *IEEE International Conference on Robotics and Automation*, 2017, pp. 5532-5538.
- [9] Connolly F, Polygerinos P, Walsh C J, et al. "Mechanical programming of soft actuators by varying fiber angle," *Soft Robotics*, vol. 2, no. 1, pp. 26-32, Mar. 2015.
- [10] Martinez R V, Fish C R, Chen X, et al. "Elastomeric origami: programmable paper-elastomer composites as pneumatic actuators," *Advanced functional materials*, vol. 22, no. 7, pp. 1376-1384, Feb. 2012.
- [11] Sun Y, Yap H K, Liang X, et al. "Stiffness Customization and Patterning for Property Modulation of Silicone-Based Soft Pneumatic Actuators," *Soft robotics*, vol. 4, no. 3, pp. 251-260, Sep. 2017.
- [12] Yang Y, Chen Y, Li Y, et al. "Bioinspired Robotic Fingers Based on Pneumatic Actuator and 3D Printing of Smart Material," *Soft robotics*, vol. 4, no. 2, pp. 147-162, Jun. 2017.
- [13] Hao Y, Wang T, Xie Z, et al. "A eutectic-alloy-infused soft actuator with sensing, tunable degrees of freedom, and stiffness properties," *Journal of Micromechanics and Microengineering*, vol. 28, no. 2, pp. 024004, Jan. 2018.
- [14] Mohammadi Nasab A, Sabzehzar A, Tatari M, et al. "A Soft Gripper with Rigidity Tunable Elastomer Strips as Ligaments," *Soft robotics*, vol. 4, no. 4, pp. 411-420, Jun. 2017.
- [15] Ozel, Selim, et al. "A precise embedded curvature sensor module for soft-bodied robots," *Sensors and Actuators A: Physical*, vol. 236, pp. 349-356, Oct. 2015.
- [16] Zhao H, O'Brien K, Li S, et al. "Optoelectronically innervated soft prosthetic hand via stretchable optical waveguides," *Science Robotics*, vol. 1, no. 1, pp. eaai7529, Dec. 2016.
- [17] Atalay A, Sanchez V, Atalay O, et al. "Batch Fabrication of Customizable Silicone Textile Composite Capacitive Strain Sensors for Human Motion Tracking," *Advanced Materials Technologies*, vol. 2, pp. 9, Jul. 2017.
- [18] Tavakoli, Mahmoud, et al. "Carbon doped PDMS: conductance stability over time and implications for additive manufacturing of stretchable electronics," *Journal of Micromechanics and Microengineering*, vol. 27, no. 3, pp. 035010, Feb. 2017.
- [19] Mengüç Y, Park Y L, Martinez-Villalpando E, et al. "Soft wearable motion sensing suit for lower limb biomechanics measurements," in *Robotics and Automation (ICRA), 2013 IEEE International Conference on. IEEE*, 2013, pp. 5309-5316.
- [20] Park Y L, Majidi C, Kramer R, et al. "Hyperelastic pressure sensing with a liquid-embedded elastomer," *Journal of Micromechanics and Microengineering*, vol. 20, no. 12, pp. 125029, Nov. 2010.
- [21] Li B, Shi Y, Hu H, et al. "Assemblies of microfluidic channels and micropillars facilitate sensitive and compliant tactile sensing," *IEEE Sensors Journal*, vol. 16, no. 24, pp. 8908-8915, Oct. 2016.
- [22] Vogt D M, Park Y L, Wood R J, et al. "Design and characterization of a soft multi-axis force sensor using embedded microfluidic channels," *IEEE sensors Journal*, vol. 13, no. 10, pp. 4056-4064, Jul. 2013.
- [23] Tiziani L O, Cahoon T W, Hammond F L, et al. "Sensorized pneumatic muscle for force and stiffness control," in *Robotics and Automation (ICRA), 2017 IEEE International Conference on. IEEE*, 2017, pp. 5545-5552.
- [24] Bilodeau R A, White E L, Kramer R K, et al. "Monolithic fabrication of sensors and actuators in a soft robotic gripper," in *Intelligent Robots and Systems (IROS), 2015 IEEE/RSJ International Conference on. IEEE*, 2015, pp. 2324-2329.
- [25] Morrow J, Shin H S, Phillips-Grafflin C, et al. "Improving soft pneumatic actuator fingers through integration of soft sensors, position and force control, and rigid fingernails," in *Robotics and Automation (ICRA), 2016 IEEE International Conference on. IEEE*, 2016, pp. 5024-5031.
- [26] Rousseau I A, Xie T. "Shape memory epoxy: Composition, structure, properties and shape memory performances," *Journal of Materials Chemistry*, vol. 20, no. 17, pp. 3431-3441, 2010.
- [27] T. L. Buckner, E. L. White, M. C. Yuen, et al. "A move-and-hold pneumatic actuator enabled by self-softening variable stiffness materials," in *Intelligent Robots and Systems (IROS), 2017 IEEE/RSJ International Conference on. IEEE*, 2017, pp. 3728-3733.
- [28] Li Wen, T M Wang, G H Wu and J H Liang. "Quantitative Thrust Efficiency of a Self-Propulsive Robotic Fish: Experimental Method and Hydrodynamic Investigation," *IEEE/ASME Transactions on Mechatronics*, vol.18, no.3, pp.1027-1038, 2013.
- [29] Ren Z, Yang X, Wang T, et al. "Hydrodynamics of a robotic fish tail: effects of the caudal peduncle, fin ray motions and the flow speed," *Bioinspiration & Biomimetics*, vol. 11, no. 1, pp.016008, 2016.
- [30] Homberg B S, Katschmann R K, Dogar M R, et al. " Haptic identification of objects using a modular soft robotic gripper , " *Intelligent Robots and Systems (IROS), 2015 IEEE/RSJ International Conference on*, 2015, pp.1698-1705.